

Resonant inversion of the circular photogalvanic effect in n -doped quantum wells

S.D. Ganichev^{†‡}, V.V. Bel'kov[‡], Petra Schneider[†], E.L. Ivchenko[‡], S.A. Tarasenko[‡],

W. Wegscheider[†], D. Weiss[†], D. Schuh[§], E.V. Beregulin[‡], and W. Prettl[†],

[†] *Fakultät Physik, University of Regensburg, 93040, Regensburg, Germany*

[‡] *A.F. Ioffe Physico-Technical Institute, 194021 St. Petersburg, Russia*

[§] *Walter Schottky Institute, TU Munich, D-85748 Garching, Germany*

(Dated: January 6, 2021)

Abstract

We show that the sign of the circular photogalvanic effect can be changed by tuning the radiation frequency of circularly polarized light. Here resonant inversion of the photogalvanic effect has been observed for direct inter-subband transition in n -type GaAs quantum well structures. This inversion of the photon helicity driven current is a direct consequence of the lifting of the spin degeneracy due to \mathbf{k} -linear terms in the Hamiltonian in combination with energy and momentum conservation and optical selection rules.

INTRODUCTION

Effects caused by spin-orbit interaction in compound semiconductor heterojunctions have been the subject of a growing number of investigations recently [1, 2]. In two-dimensional systems based on quantum wells (QWs) the electron spin couples to the electron motion and results, under optical orientation with circularly polarized light, in spin photocurrents [3]. The direction and magnitude of this spin photocurrent depend on the degree of circular polarization of the incident light [4]. This phenomenon belongs to the class of photogalvanic effects [5] and represents here a circular photogalvanic effect (CPGE).

It was shown in [3] that the CPGE in zinc-blende structure based QWs is caused by spin orientation of carriers in systems where the spin degeneracy of the band structure is lifted by \mathbf{k} -linear terms in the Hamiltonian [6, 7]. In this case homogeneous irradiation of QWs with circularly polarized light results in an asymmetric distribution of photo-excited carriers in \mathbf{k} -space which leads to the current. So far this effect has been observed only for indirect intra-subband transitions in n - and p -type QWs (Drude absorption) and for direct inter-subband heavy-hole - light-hole transitions in p -type QWs [3, 8].

Here we report on the first observation of a resonant inversion of the CPGE at direct transitions between size quantized subbands in n -type QWs. This effect demonstrates in a very direct way the spin splitting of subbands in \mathbf{k} -space in zero electric and magnetic field due to spin-orbit interaction. We show that the sign of the spin driven circular photogalvanic current can be reversed by tuning the radiation frequency. This inversion of the photon helicity driven current is a direct consequence of \mathbf{k} -linear terms in the subband structure in combination with conservation laws and optical selection rules.

EXPERIMENTAL RESULTS

Direct inter-subband transitions between the lowest ($e1$) and the second ($e2$) conduction subband in n -type GaAs QWs have been obtained by applying a line tunable pulsed transversely excited atmospheric pressure (TEA)-CO₂ laser. The laser yields strong linearly polarized emission at wavelengths λ between 9.2 μm and 10.8 μm corresponding to photon energies $\hbar\omega$ ranging from 135 meV to 114 meV. The quantum well widths were chosen to be ≈ 8 nm, so that the separation of the subbands $e1$ and $e2$ matches the photon energy range of the laser [9, 10]. Molecular-beam-epitaxy grown (001)- and (113)-oriented n -type GaAs/AlGaAs QW samples of 8.8 nm, 8.2 nm and 7.6 nm width with free-carrier densities ranging between $2 \cdot 10^{11} \text{ cm}^{-2}$ and $1 \cdot 10^{12} \text{ cm}^{-2}$ were investigated at room temperature. The (113)-oriented samples have been grown on GaAs (113)A substrates employing growth conditions under which Si dopants are predominantly incorporated as donors [11] as confirmed by Hall measurements.

On each sample a pair of contacts along a line parallel to the x -direction has been attached (see Fig. 1c). We use Cartesian coordinates for (001)-oriented samples $x \parallel [1\bar{1}0]$, $y \parallel [110]$, $z \parallel [001]$ and for (113)-oriented samples $x' = x \parallel [1\bar{1}0]$, $y' \parallel [3\bar{3}\bar{2}]$, $z' \parallel [113]$. Right handed (σ_+) and left handed (σ_-) circularly polarized radiation was achieved by using a Fresnel rhomb. In order to correlate the spectral dependence of the CPGE current to the absorption of the QWs, optical transmission measurements were carried out using a Fourier transform infrared spectrometer. The current j generated by circularly polarized light in the unbiased devices was measured via the voltage drop across a 50 Ω load resistor in a closed circuit configuration (see Fig. 1c). The voltage in response to a laser pulse was recorded with a storage oscilloscope.

Illuminating the unbiased QW structures with circularly polarized radiation results in a current signal due to CPGE which is proportional to the helicity P_{circ} of the radiation. The signal follows the temporal structure of the laser pulse and changes sign if the circular polarization is switched from σ_+ to σ_- . Typical signal traces are shown in Fig. 1 compared to records of a linear photon drag detector [12]. In (001)-oriented samples, belonging to the point group C_{2v} , the CPGE current is only observed

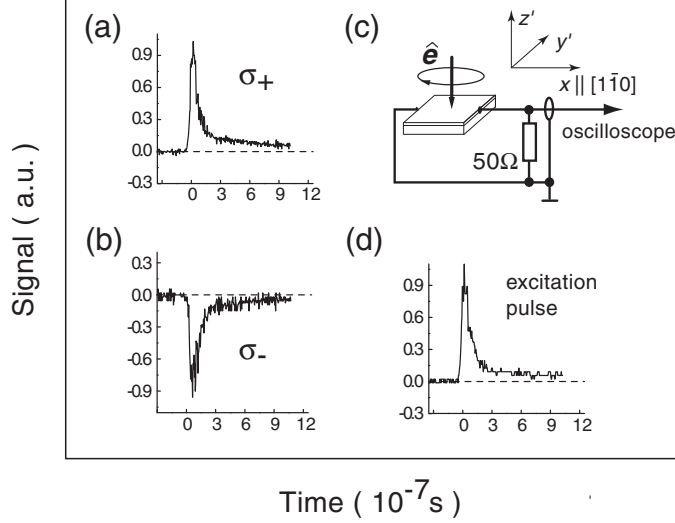


FIG. 1: Oscillographic traces obtained through excitation with $\lambda = 10.6 \mu\text{m}$ radiation of (113)-grown n -GaAs QWs. (a) and (b) show CPGE signals obtained for σ_+ and σ_- -circular polarization, respectively. For comparison in (d) a signal pulse of a fast photon drag detector is plotted. In (c) the measurement arrangement is sketched. For (113)-grown samples being of C_s symmetry radiation was applied at normal incidence and the current was detected in the direction $x \parallel [1\bar{1}0]$. For (001)-grown QWs oblique incidence with light propagating along $[110]$ direction was used and the current was detected in $x \parallel [1\bar{1}0]$ direction.

under oblique incidence of radiation, as expected from symmetry [3]. For illumination along y -direction the helicity dependent photocurrent flows in x -direction perpendicular to the wavevector of the incident light. This is observed in experiment. In Fig. 2 the photocurrent as a function of photon energy is plotted for σ_+ and σ_- polarized radiation together with the absorption spectrum. The data are presented for a (001)-grown n -GaAs QW of 8.2 nm width measured at room temperature. The current for both, left and right handed circular polarizations, changes sign at a frequency $\omega = \omega_{inv}$. This inversion frequency ω_{inv} coincides with the frequency of the absorption peak (see Fig. 2). The absorption peak frequency and ω_{inv} depend on the sample width according to the variation of the subband energy separation. This has been verified by measuring QWs of different widths. Spin orientation induced CPGE and its spectral sign inversion

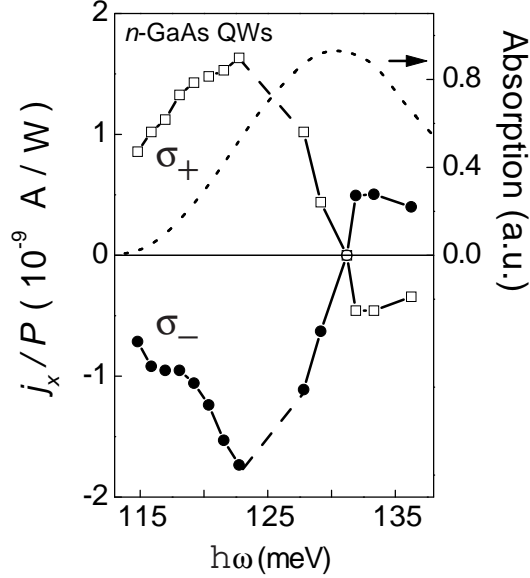


FIG. 2: Photocurrent in QWs normalized by the light power P as a function of the photon energy $\hbar\omega$. Measurements are presented for n -type (001)- grown GaAs/AlGaAs QWs of 8.2 nm width (symmetry class C_{2v}) at $T = 293$ K. Oblique incidence of σ_+ (squares) and σ_- (circles) circular polarized radiation with an angle of incidence $\Theta_0 = 20^\circ$ was used. The current j_x was measured perpendicular to the direction of light propagation y . The dotted line shows the absorption measurement using a Fourier transform infrared spectrometer.

have also been detected in a (113)-oriented n -GaAs QW which belongs to the point group C_s . In this case the helicity dependent signal is observed in x -direction at normal incidence of radiation along z' .

MICROSCOPIC MODEL

The physical origin of the effect is sketched in Fig. 3 for C_s symmetry and in Fig. 4 for C_{2v} symmetry. For both symmetries the degeneracy in \mathbf{k} -space is lifted. First we consider the simplest case of C_s symmetry relevant for (113)-oriented samples. The $\sigma_{z'}k_x$ contribution to the Hamiltonian, responsible for the effect under normal incidence, splits the electron spectrum into spin sub-levels with the spin components $s = \pm 1/2$ along the growth direction z' . As a result of optical selection rules right-handed circu-

lar polarization under normal incidence induces direct optical transitions between the subband $e1$ with spin $s = -1/2$ and $e2$ with spin $s = +1/2$. For monochromatic radiation optical transitions occur only at a fixed k_x where the energy of the incident light matches the transition energy as is indicated by the arrow in Fig. 3a. Therefore optical transitions induce an imbalance of momentum distribution in both subbands yielding an electric current. However, a non-equilibrium distribution of carriers in the upper subband rapidly relaxes due to the very effective relaxation channel of LO -phonons emission, because the energy separation ε_{21} between $e1$ and $e2$ at $k_x = 0$ is well above the energy of LO phonons in n -GaAs QWs ($\varepsilon_{LO} = 35.4$ meV). Therefore the contribution of the $e2$ subband to the electric current vanishes and the magnitude and direction of electron flow is determined by the momentum distribution of carriers in the lowest subband.

Fig. 3a and 3b show what happens when, as in our experiment, the energy of the incident light is varied from energies above ε_{21} to values below ε_{21} . Here ε_{21} is the subbands' energy separation at $\mathbf{k}=0$. At large photon energy, $\hbar\omega > \varepsilon_{21}$, excitation occurs at positive k_x resulting in a current j_x shown by arrow in Fig. 3a. A reduced photon frequency shifts the transition towards negative k_x and reverses the direction of the current (Fig. 3b). The inversion of the current's sign occurs at a photon frequency ω_{inv} corresponding to the transition at the minimum of $e1$ ($s=-1/2$). The model suggests that the magnitude of the spin splitting described by the Rashba and Dresselhaus terms [6, 7] could easily be derived from the energy shift $\hbar\omega_{inv} - \varepsilon_{21}$. However, our measurements show, that the inhomogeneous broadening of the optical transition in real QWs is too large to obtain this energy shift. On the other hand the model clearly shows that without \mathbf{k} -linear terms in the band structure neither an inversion nor a current would exist. Similar arguments hold for C_{2v} symmetry (relevant for (001)-oriented samples) under oblique incidence (see Fig. 4) although the simple selection rules are no longer valid [13]. This is pointed out in more detail at the end of the next section.

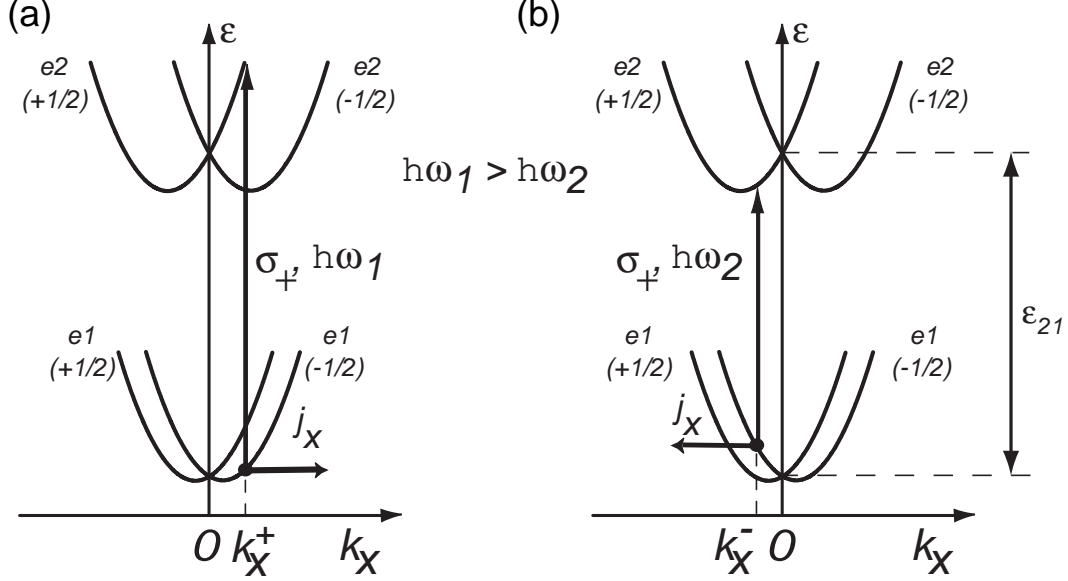


FIG. 3: Microscopic picture describing the origin of the inversion of the photocurrent in C_s point group samples. The essential ingredient is the splitting of the conduction band due to \mathbf{k} -linear terms. Right handed circularly polarized radiation, σ_+ , induces direct spin-flip transitions (vertical arrows) from $e1$ subband with $s = -1/2$ to $e2$ subband with $s = +1/2$. As a result an unbalanced occupation of the k_x states occurs yielding a spin polarized photocurrent. (a) For transitions with k_x^+ right to the minimum of $e1$ ($s=-1/2$) subband the current indicated by j_x is positive. (b) At smaller $\hbar\omega$ the transition occurs at k_x^- , now left to the subband minimum, and the current reverses its sign.

MICROSCOPIC THEORY

The theory of the circular photogalvanic effect is developed by using the spin density matrix technique [5]. Generally the total electric current that appears in a structure under inter-subband excitation consists of the contributions from the $e1$ and $e2$ subbands

$$\mathbf{j} = \mathbf{j}^{(1)} + \mathbf{j}^{(2)}, \quad (1)$$

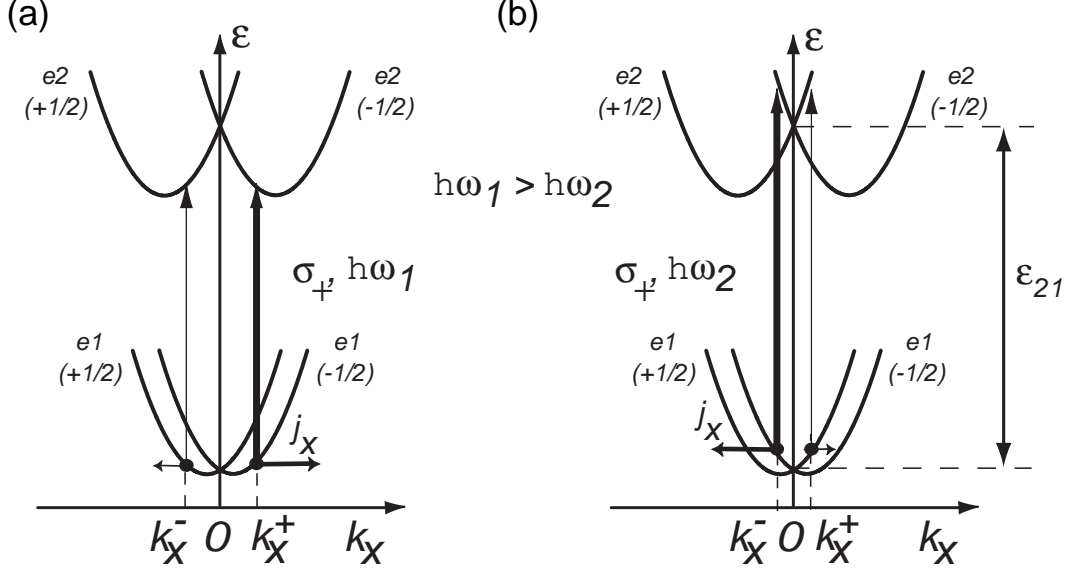


FIG. 4: Microscopic picture describing the origin of the inversion of the photocurrent in C_{2v} point group samples. (a) Excitation with σ_+ radiation of $\hbar\omega$ less than the energy subband separation ε_{21} induces direct spin-conserving transitions (vertical arrows) at k_x^- and k_x^+ . The rates of these transitions are different as illustrated by different thickness of the arrows (reversing the angle of incidence mirrors the transition rates). This leads to a photocurrent due to an asymmetrical distribution of carriers in \mathbf{k} -space if the splitting of the $e1$ and $e2$ subbands are non-equal. (b) Increasing of the photon energy shifts more intensive transitions to the left and less intensive to the right resulting in a current sign change.

which in the relaxation time approximation are given by standard expressions

$$\mathbf{j}^{(\nu)} = e \sum_{\mathbf{k}} \tau_p^{(\nu)} \text{Tr} \left[\hat{\mathbf{v}}^{(\nu)}(\mathbf{k}) \dot{\rho}^{(\nu)}(\mathbf{k}) \right]. \quad (2)$$

Here e is the electron charge, $\nu=1,2$ labels the subband $e\nu$, $\tau_p^{(\nu)}$ is the momentum relaxation time in the subband $e\nu$, $\dot{\rho}^{(\nu)}(\mathbf{k})$ is the generation of the density matrix and $\hat{\mathbf{v}}^{(\nu)}$ is the velocity operator in the subband given by

$$\hat{\mathbf{v}}^{(\nu)} = \hbar^{-1} \nabla_{\mathbf{k}} \hat{H}^{(\nu)}. \quad (3)$$

For the sake of simplicity we will consider a parabolic electron spectrum for the subbands and take a Hamiltonian of the form

$$\hat{H}^{(\nu)} = \varepsilon^{(\nu)} + \frac{\hbar^2 \mathbf{k}^2}{2m^*} + \hat{\mathcal{H}}_{1\mathbf{k}}^{(\nu)}, \quad (4)$$

where $\varepsilon^{(\nu)}$ is the energy of size-quantization, $\hat{\mathcal{H}}_{1\mathbf{k}}^{(\nu)}$ is the spin-dependent \mathbf{k} -linear contribution, and m^* is the effective mass equal for both subbands.

It is convenient to write the generation matrices in the basis of spin eigenstates $\chi_{\nu\mathbf{k}s}$ of the Hamiltonians $\hat{H}^{(\nu)}$. For the case of inter-subband transitions $e1 \rightarrow e2$ the corresponding equations have the form (see [14])

$$\begin{aligned} \dot{\rho}_{ss'}^{(1)}(\mathbf{k}) &= -\frac{\pi}{\hbar} \sum_{s_1} \mathcal{M}_{s_1, s'}(\mathbf{k}) \mathcal{M}_{s_1, s}^*(\mathbf{k}) \times \\ & [f_{\mathbf{k}s} \delta(\varepsilon_{2\mathbf{k}s_1} - \varepsilon_{1\mathbf{k}s} - \hbar\omega) + f_{\mathbf{k}s'} \delta(\varepsilon_{2\mathbf{k}s_1} - \varepsilon_{1\mathbf{k}s'} - \hbar\omega)] , \\ \dot{\rho}_{ss'}^{(2)}(\mathbf{k}) &= \frac{\pi}{\hbar} \sum_{s_1} f_{\mathbf{k}s_1} \mathcal{M}_{s, s_1}(\mathbf{k}) \mathcal{M}_{s', s_1}^*(\mathbf{k}) \times \\ & [\delta(\varepsilon_{2\mathbf{k}s} - \varepsilon_{1\mathbf{k}s_1} - \hbar\omega) + \delta(\varepsilon_{2\mathbf{k}s'} - \varepsilon_{1\mathbf{k}s_1} - \hbar\omega)] , \end{aligned} \quad (5)$$

Here s , s' and s_1 are the spin indices, $f_{\mathbf{k}s}$ is the equilibrium distribution function in the subband $e1$ (the subband $e2$ is empty in equilibrium), $\varepsilon_{\nu\mathbf{k}s}$ is the electron energy, and $\mathcal{M}_{s_1, s}(\mathbf{k})$ is the matrix element of inter-subband optical transitions ($e1, \mathbf{k}, s$) \rightarrow ($e2, \mathbf{k}, s_1$). The latter is given by $\mathcal{M}_{s, s_1}(\mathbf{k}) = \chi_{2\mathbf{k}s}^\dagger \hat{M} \chi_{1\mathbf{k}s_1}$, where \hat{M} is a 2×2 matrix describing the inter-subband transitions in the basis of fixed spin states $s_z = \pm 1/2$,

$$\hat{M} = -\frac{eA}{cm^*} p_{21} \begin{bmatrix} e_z & \Lambda(e_x - ie_y) \\ -\Lambda(e_x + ie_y) & e_z \end{bmatrix}, \quad (6)$$

A is the amplitude of the electro-magnetic wave related to light intensity by $I = A^2 \omega^2 n_\omega / (2\pi c)$, \mathbf{e} is the unit vector of the light polarization, n_ω is the refraction index of the media, c is the light velocity, and p_{21} is the momentum matrix element between the envelope functions of size quantization $\varphi_1(z)$ and $\varphi_2(z)$ in the subbands $e1$ and $e2$,

$$p_{21} = -i\hbar \int \varphi_2(z) \frac{\partial}{\partial z} \varphi_1(z) dz. \quad (7)$$

The parameter Λ originates from $\mathbf{k} \cdot \mathbf{p}$ admixture of valence band states to the electron wave function and is given by

$$\Lambda = \frac{\varepsilon_{21}\Delta(2\varepsilon_g + \Delta)}{2\varepsilon_g(\varepsilon_g + \Delta)(3\varepsilon_g + 2\Delta)}, \quad (8)$$

where ε_g is the energy of the band gap, and Δ is the energy of spin-orbit splitting of the valence band. As one can see from Eq. (6), the parameter Λ determines the absorbance for the light polarized in the interface plane.

In ideal QWs the circular photocurrent \mathbf{j} may be obtained from Eqs. (1)-(5). However, in real structures the spectral width of the inter-subband resonance is broadened due to fluctuation of the QW width and hence exceeds the spectral width of the absorption spectrum of an ideal structure. The inhomogeneous broadening can be taken into account assuming that the energy separation between subbands ε_{21} varies in the QW plane. Then by convolution of the photocurrent $\mathbf{j}(\varepsilon_{21})$ with the distribution function $F(\varepsilon_{21})$ we obtain

$$\bar{\mathbf{j}} = \int \mathbf{j}(\varepsilon_{21}) F(\varepsilon_{21}) d\varepsilon_{21}. \quad (9)$$

The function $F(\varepsilon_{21})$ for inhomogeneous broadening may be expanded in powers of $\varepsilon_{21} - \hbar\omega$ and by considering only the first two terms we obtain

$$F(\varepsilon_{21}) \approx F(\hbar\omega) + F'(\hbar\omega)(\varepsilon_{21} - \hbar\omega). \quad (10)$$

Taking into account the Hamiltonian $\hat{\mathcal{H}}_{1\mathbf{k}}^{(\nu)}$ to be linear in \mathbf{k} , the averaged current is finally given by

$$\begin{aligned} \bar{\mathbf{j}} = en_e \frac{\pi}{\hbar^2} & \left[\tau_p^{(2)} F(\hbar\omega) + (\tau_p^{(1)} - \tau_p^{(2)}) F'(\hbar\omega) \bar{\varepsilon} \right] \times \\ & \text{Tr} \left[\hat{M}^\dagger \left(\nabla_{\mathbf{k}} \hat{\mathcal{H}}_{1\mathbf{k}}^{(2)} \right) \hat{M} - \hat{M} \left(\nabla_{\mathbf{k}} \hat{\mathcal{H}}_{1\mathbf{k}}^{(1)} \right) \hat{M}^\dagger \right], \end{aligned} \quad (11)$$

where n_e is the 2D carrier density, and $\bar{\varepsilon}$ is the mean value of the electron energy. For a degenerate 2D electron gas $\bar{\varepsilon} = \varepsilon_F/2$ and for a non-degenerate gas $\bar{\varepsilon} = k_B T$, where ε_F is the Fermi energy, k_B is the Boltzmann constant and T is the temperature. We note, that the distribution function $F(\hbar\omega)$ determines the spectral behaviour of the absorbance in the presence of an inhomogeneous broadening.

C_s- symmetry and normal incidence.

In (113)-grown QW structures of C_s symmetry the CPGE occurs under normal incidence of the radiation. In this case the \mathbf{k} -linear contribution to the Hamiltonian responsible for the effect is given by $\beta_{z'x}^{(\nu)}\sigma_{z'}k_x$. Here $\beta_{z'x}^{(\nu)}$ are the coefficients being different for the $e1$ - and $e2$ subbands. The \mathbf{k} -linear term splits the electron spectrum into spin sub-levels with the spin components $s = \pm 1/2$ along the growth direction z' (see Fig. 3). Thus the electron parabolic dispersion in the subbands $e1$ and $e2$ has the form

$$\varepsilon_{\nu,\mathbf{k},\pm 1/2} = \varepsilon^{(\nu)} + \frac{\hbar^2 (k_x^2 + k_{y'}^2)}{2m^*} \pm \beta_{z'x}^{(\nu)}k_x. \quad (12)$$

For direct inter-subband transitions under normal incidence selection rules allow only the spin-flip transitions, $(e1, -1/2) \rightarrow (e2, 1/2)$ for σ_+ photons and $(e1, 1/2) \rightarrow (e2, -1/2)$ for σ_- photons [13]. Due to these selection rules together with energy and momentum conservation laws the optical inter-subband transition under, for example, σ_+ photoexcitation is only allowed for the fixed wavevector k_x given by

$$k_x = \frac{\hbar\omega - \varepsilon_{21}}{\beta_{z'x}^{(2)} + \beta_{z'x}^{(1)}}. \quad (13)$$

Velocities of electrons in the $e2$ subband and of 'holes' in the $e1$ subband generated by this transition are given by

$$v_x^{(1)} = \hbar k_x / m^* - \beta_{z'x}^{(1)} / \hbar, \quad v_x^{(2)} = \hbar k_x / m^* + \beta_{z'x}^{(2)} / \hbar, \quad (14)$$

This unbalanced distribution of carriers in \mathbf{k} -space induces an electric current

$$j_x = j_x^{(1)} + j_x^{(2)} = -e \frac{\eta_{\parallel} I}{\hbar\omega} \left(v_x^{(1)} \tau_p^{(1)} - v_x^{(2)} \tau_p^{(2)} \right) P_{circ}, \quad (15)$$

where I is the light intensity and η_{\parallel} is the absorbance or the fraction of the energy flux absorbed in the QW due to the inter-subband transitions under normal incidence. Note that the magnitude of the photocurrent $j_x^{(2)}$, corresponding to the second term in the bracket of Eq. (15), and stems from photoelectrons in the $e2$ subband is smaller than $|j_x^{(1)}|$ because $\tau_p^{(2)} < \tau_p^{(1)}$ as described above. The resonant inversion of the circular

photocurrent is clearly seen from Eqs. (13) - (15) because η_{\parallel} is positive and $v_x^{(\nu)}$ changes its sign at a particular frequency.

For a degenerate 2D electron gas at low temperature we find that the dependence of the absorbance η_{\parallel} on $\hbar\omega$ and $\beta_{z'x}^{(\nu)}$ is given by

$$\frac{\eta_{\parallel}}{\hbar\omega} \propto \frac{1}{|\beta_{z'x}^{(2)} + \beta_{z'x}^{(1)}|} \left[\tilde{\varepsilon}_F - \frac{\hbar^2}{2m^*} \left(\frac{\hbar\omega - \varepsilon_{21}}{\beta_{z'x}^{(2)} + \beta_{z'x}^{(1)}} \right)^2 \right]^{1/2}, \quad (16)$$

where $\tilde{\varepsilon}_F = \varepsilon_F - m^*[\beta_{z'x}^{(1)}/(\sqrt{2}\hbar)]^2$.

Taking into account the inhomogeneous broadening we finally obtain for the averaged circular photocurrent

$$\bar{j}_x = \frac{e}{\hbar} (\beta_{z'x}^{(2)} + \beta_{z'x}^{(1)}) \left[\tau_p^{(2)} \bar{\eta}_{\parallel}(\hbar\omega) + (\tau_p^{(1)} - \tau_p^{(2)}) \bar{\varepsilon} \frac{d\bar{\eta}_{\parallel}(\hbar\omega)}{d\hbar\omega} \right] \frac{IP_{circ}}{\hbar\omega}, \quad (17)$$

where $\bar{\eta}_{\parallel} \propto F(\hbar\omega)$ is the calculated absorbance neglecting \mathbf{k} -linear terms but taking into account the inhomogeneous broadening.

C_{2v} symmetry and oblique incidence.

In the case of C_{2v} point symmetry which is relevant for (001)-oriented QWs the current flows only at oblique incidence and is caused by \mathbf{k} -linear contributions to the electron effective Hamiltonian given by

$$\mathcal{H}_{1\mathbf{k}}^{(\nu)} = \beta_{xy}^{(\nu)} \sigma_x k_y + \beta_{yx}^{(\nu)} \sigma_y k_x. \quad (18)$$

The coefficients $\beta_{xy}^{(\nu)}$ and $\beta_{yx}^{(\nu)}$ are related to the bulk-inversion asymmetry (BIA) or Dresselhaus term [7] and structure-inversion asymmetry (SIA) or Rashba term [6] by

$$\beta_{xy}^{(\nu)} = \beta_{BIA}^{(\nu)} + \beta_{SIA}^{(\nu)}, \quad \beta_{yx}^{(\nu)} = \beta_{BIA}^{(\nu)} - \beta_{SIA}^{(\nu)}. \quad (19)$$

The circular photocurrent due to inter-subband transition in (001)-grown QWs in the presence of inhomogeneous broadening can be calculated following Eq. (11) yielding

$$j_x = -\Lambda \frac{e}{\hbar} (\beta_{yx}^{(2)} - \beta_{yx}^{(1)}) \left[\tau_p^{(2)} \eta_{\perp}(\hbar\omega) + (\tau_p^{(1)} - \tau_p^{(2)}) \bar{\varepsilon} \frac{d\eta_{\perp}(\hbar\omega)}{d\hbar\omega} \right] \frac{IP_{circ}}{\hbar\omega} \hat{e}_y \quad (20)$$

where $\hat{\mathbf{e}}$ is the unit vector directed along the light propagation and η_{\perp} is the absorbance for the polarization perpendicular to the QW plane. The current in y -direction can be obtained by interchanging the indices x and y in Eq. (20).

The origin of the spin orientation induced CPGE caused by direct inter-subband transitions in C_{2v} -symmetry systems is illustrated in Fig. 4 for σ_{+} radiation. In C_{2v} -symmetry the $\sigma_y k_x$ contribution to the Hamiltonian splits the subbands in k_x direction in two spin branches with $s = \pm 1/2$ oriented along y (see Fig. 4). Due to selection rules the absorption of circularly polarized radiation is spin-conserving [5]. The asymmetric distribution of photo-excited electrons resulting in a current is caused by these spin-conserving but spin-dependent transitions (see Eq. (20)). This is in contrast to spin-flip processes occurring in (113)-grown QWs described above. It turns out that under oblique excitation by circularly polarized light the rates of inter-subband transitions are different for electrons with the spin oriented co-parallel and antiparallel to the in-plane direction of light propagation [15]. The difference is proportional to the product $|M_{\parallel} M_{\perp}|$, where M_{\parallel} and M_{\perp} are the absorption matrix elements for in-plane and normal light polarization. This is depicted in Fig. 4 by vertical arrows of different thickness. In systems with \mathbf{k} -linear spin splitting such processes lead to an asymmetrical distribution of carriers in \mathbf{k} -space, i.e. to an electrical current. Similar to C_s symmetry the variation of the photon energy leads to the inversion of the current direction (see Fig. 4a and 4b). Since the circular photogalvanic effect in QW structures of C_{2v} symmetry is caused by spin-dependent *spin-conserving* optical transitions, the photocurrent described by Eq. (20) in contrast to Eq. (17) is proportional to the difference of subband spin splittings.

CONCLUSIONS

Our experiments show that direct inter-subband transitions in n -type GaAs QWs result in a spin orientation induced CPGE. The central observation is a change of the sign of the CPGE current close to resonance of inter-subband transitions. The theoretical results give a detailed description of all features observed in experiment.

The sign inversion follows for C_s symmetry from Eq. (17) and for C_{2v} symmetry from Eq. (20). If $\tau_p^{(2)} \ll \tau_p^{(1)}$ the first term on the right hand side in square brackets of both equations is vanishingly small compared to the second one. Therefore the photocurrent is proportional to the derivative of the absorbance and is zero at the frequency of the absorption peak as observed in experiment. Thus the assumption that the momentum relaxation in the upper subband is much faster than in the lower subband is satisfied.

Comparing theory with experiment we also note that for C_{2v} symmetry the spin splitting in \mathbf{k} -space is different for the $e1$ and $e2$ subbands. Eq. (20) shows that for equal spin splitting, $\beta_{yx}^{(2)} = \beta_{yx}^{(1)}$, the current vanishes. For C_s symmetry in contrast, the spin-orientation induced CPGE current is proportional to the sum of the subband spin splittings and therefore exist for $\beta_{yx}^{(2)} = \beta_{yx}^{(1)}$. The observation of the CPGE for direct inter-subband transitions allows to extend the method of spin-sensitive bleaching, previously demonstrated for p -type QWs [16], and therefore to investigate electron spin relaxation times in n -type QWs for monopolar spin orientation [16, 17].

We acknowledge financial support from the DFG, the RFBR and the programs of the RAS.

-
- [1] S.A. Wolf, D.D. Awschalom, R.A. Buhrman, J.M. Daughton, S. von Molnar, M.L. Roukes, A.Y. Chtchelkanova, and D.M. Treger, *Science* **294**, 1488 (2001).
- [2] *Semiconductor Spintronics and Quantum Computation*, eds. D.D. Awschalom, D. Loss, and N. Samarth, in the series *Nanoscience and technology*, eds. K. von Klitzing, H. Sakaki, and R. Wiesendanger (Springer, Berlin, 2002).
- [3] S.D. Ganichev, E. L. Ivchenko, S.N. Danilov, J. Eroms, W. Wegscheider, D. Weiss, and W. Prettl, *Phys. Rev. Lett.* **86**, 4358 (2001).
- [4] S.D. Ganichev, E.L. Ivchenko, H. Ketterl, W. Prettl, and L.E. Vorobjev, *Appl. Phys. Lett.* **77**, 3146 (2000).
- [5] E.L. Ivchenko, and G.E. Pikus, *Superlattices and Other Heterostructures. Symmetry and Optical Phenomena*, (Springer, Berlin 1997).
- [6] Y.A. Bychkov, and E.I. Rashba, *Pis'ma ZhETF* **39**, 66 (1984) [*Sov. JETP Lett.* **39**, 78 (1984)].
- [7] M.I. D'yakonov, and V.Yu. Kachorovskii, *Fiz. Tekh. Poluprov.* **20**, 178 (1986) [*Sov. Phys. Semicond.* **20**, 110 (1986)].
- [8] S.D. Ganichev, E.L. Ivchenko, and W. Prettl, *Physica E* **14**, 166 (2002).
- [9] W. Hilber, M. Helm, K. Alavi, and R. N. Pathak, *Superlattices and Microstructures* **21**, 85 (1997).
- [10] S. Tsujino, M. Rufenacht, H. Nakajima, T. Noda, C. Metzner, and H. Sakaki, *Phys. Rev. B* **62**, 1560 (2000).
- [11] N. Sakamoto, K. Hirakawa, and T. Ikoma, *Appl. Phys. Lett.* **67**, 1444 (1995).
- [12] S.D. Ganichev, Ya.V. Terent'ev, and I.D. Yaroshetskii, *Pis'ma Zh. Tekh. Phys.* **11**, 46 (1985) [*Sov. Tech. Phys. Lett.* **11**, 20 (1985)].
- [13] R.J. Warburton, C. Gauer, A. Wixforth, and J.P. Kotthaus, B. Brar, and H. Kroemer, *Phys. Rev. B* **53**, 7903 (1996).
- [14] E.L. Ivchenko, Yu.B. Lyanda-Geller, and G.E. Pikus, *Zh. Exp. Teor. Fiz.* **98**, 989 (1990) [*Soviet Physics - JETP* **71**, 550 (1990)].

- [15] E.L. Ivchenko, S.A. Tarasenko, JETP, to be published.
- [16] S.D. Ganichev, S.N. Danilov, V.V. Bel'kov, E.L. Ivchenko, M. Bichler, W. Wegscheider, D. Weiss, and W. Prettl, Phys. Rev. Lett. **88**, 057401-1 (2002).
- [17] S.D. Ganichev, E.L. Ivchenko, V.V. Bel'kov, S.A. Tarasenko, M. Sollinger, D. Weiss, W. Wegscheider, and W. Prettl, *Nature* (London) **417**, 153 (2002).